

A Study on the Electronic Properties of Passive Film Formed on Fe-20Cr by Photoelectrochemical and Mott-Schottky Analysis

EunAe Cho and HyukSang Kwon*

Fuel Cell Research Center, Korea Institute of Science and Technology
P.O.BOX 131, CheongRyang, Seoul, Korea, 130-650

*Dept. of Materials Science and Engineering, Korea Advanced Institute of Science and Technology
73-1, KuSongDong, YuSongGu, TaeJon, Korea, 305-701

The electronic properties of passive film formed on Fe-20Cr stainless steel in pH 8.5 buffer solution were examined by the photocurrent measurements and Mott-Schottky analysis of the film. The passive film on Fe-20Cr exhibited an amorphous or highly disordered n-type semiconductor. The photocurrent spectrum for the passive films formed on Fe-20Cr was almost same in shape to that for the passive film of Fe except for the large difference in photocurrent intensity, which demonstrated that the passive film on Fe-20Cr is composed of Cr substituted γ -Fe₂O₃. However, the large difference in photocurrent intensity for passive film between Fe and Fe-20Cr was due presumably to the fact that Cr³⁺ ions in passive film act as effective recombination sites of electron-hole pairs. The relatively high intensity of photocurrent and two linear regions on Mott-Schottky plot for the passive film formed at potentials in Cr-transpassive region was associated with Cr⁶⁺ ions present in the film.

Keywords : passive film, stainless steels, electronic properties, photocurrent, Mott-Schottky plot

1. Introduction

The excellent corrosion resistance of stainless steels is largely due to the protective passive film formed on the surface. Elucidating the nature of the passive film is a prerequisite for understanding such a high corrosion resistance of stainless steels. Many analytical studies have agreed that the passive film on Fe-Cr stainless steels consists of Cr-enriched (Fe, Cr) oxide/hydroxide,¹⁻⁶⁾ although there is still some controversy as to the detailed structure and composition of the passive film. The extreme complexity of the metal/passive film/electrolyte system of stainless steels makes the clarification of the passive film difficult.

The electronic structure of the passive film is an important issue in that ionic movement in the passive film is driven by the electric field, which is in turn affected by the electronic structure.⁷⁾ In this way, the electronic structure is closely related to corrosion phenomena including film breakdown and pitting initiation.⁸⁾ Recently, photocurrent analysis and Mott-Schottky analysis via impedance measurements for the passive film have been employed to examine the *in situ* electronic properties of the passive film.

In spite of intensive studies using the photocurrent and

Mott-Schottky analyses,^{6),9)} the electronic structure of the passive film on stainless steels still remains obscure. Difficulties in interpreting the electronic structure of the film arise from high doping levels, deep traps, presence of surface states, and complicated structure of the passive film. Hakiki et al.⁶⁾ proposed that passive film formed on Fe-Cr stainless steels in pH 9.2 borate buffer solution has a duplex-layered structure of inner p-type chromium oxide and outer n-type iron oxide, and hence that the electronic structure of the passive film is a p-n heterojunction. On the other hand, Bojinov et al.⁹⁾ suggested based on the point defect model⁷⁾ that the passive film is a heavily doped n-type semiconductor/insulator/p-type semiconductor (n-i-p) junction.

Many researchers have attempted to determine the structure and composition of passive film on stainless steels by analyzing the electronic properties of the film through the photocurrent and impedance measurement.¹⁰⁻¹⁴⁾ Fujimoto et al.¹⁰⁾ proposed that the passive film on Fe-8-18Cr alloys in 0.1 M H₂SO₄ solution consists of inner Cr₂O₃ with band gap energy (E_g) of 3.6 eV and outer Cr(OH)₃ with E_g of 2.5 eV. However, most of the researchers analyzed the electronic structure of passive film on Fe-Cr alloys by regarding the film as a single-layered oxide. Sunseri et al.¹¹⁾ and Di Paola et al.¹²⁾

reported that the passive film formed on ferritic stainless steels in 3.5 % NaCl solution was a $\text{Cr}_2\text{O}_3\text{-Fe}_2\text{O}_3$ solid solution with E_g ranging from 1.9 to 2.8 eV (depending on the ratio of Cr_2O_3 to Fe_2O_3 and film formation potential). Klopper et al.¹³⁾ suggested that the structure of passive film formed on Fe-5~30Cr alloys in neutral borate buffer solution resembles that of a $\alpha\text{-Fe}_2\text{O}_3$ with E_g of 1.9 eV. Simoes et al.¹⁴⁾ proposed that the passive film on type 304 stainless steel in pH 9.2 borate buffer solution consisted of Cr-substituted Fe-oxide with E_g of 2.7~2.9 eV.

Research objective of the present work is to characterize the physical and electronic structure of the passive film formed on Fe-20Cr ferritic stainless steel in a borate buffer solution by examining the influences of film formation potential on the semiconducting properties of the film using the photo-electrochemical spectroscopy and electrochemical impedance spectroscopy.

2. Experimental

High purity Fe-20 wt.% Cr alloy (Fe-20Cr) was used as a working electrode. A conventional three electrode cell of 1 L-multi neck flask with a quartz window as a photon inlet was used for the photocurrent and impedance measurements. The cell was equipped with a platinum counter electrode and a saturated calomel reference electrode (SCE). The procedures for sample preparation and the experimental arrangement were described in detail previously.¹⁵⁾ All the experiments were carried out at room temperature in deaerated pH 8.5 buffer solution. Passive film on Fe-20Cr was prepared by polarization at potentials of 0 to 800 mV_{SCE} for about 24 hrs. The 300 W Xenon arc lamp combined with a scanning digital monochromator was used to impose a monochromatic illumination to the working electrode. The monochromator was controlled at a scanning rate of 1 nm/s by stepping motor, which made it possible to provide monochromatic photons with 200 to 800 nm wavelengths to the working electrode. To increase the photon flux, white light from the Xe lamp was focused to the light inlet using two auxiliary focusing lenses. The capacitance measurements for the Mott-Schottky analysis were conducted on the passive films formed on Fe-20Cr for 1 hr at various potentials ranging from -100 mV_{SCE} to 900 mV_{SCE}, by sweeping the applied potential in negative direction from the film formation potential with excitation voltage of 10 mV (peak-to-peak) using a Frequency Response Analyzer. The imaginary part of the impedance (Z'') was measured as a function of the applied potential, and the corresponding capacitance of space charge layer (C_{sc}) was obtained from $C_{sc} = -1/\omega Z''$, where ω is the angular frequency.

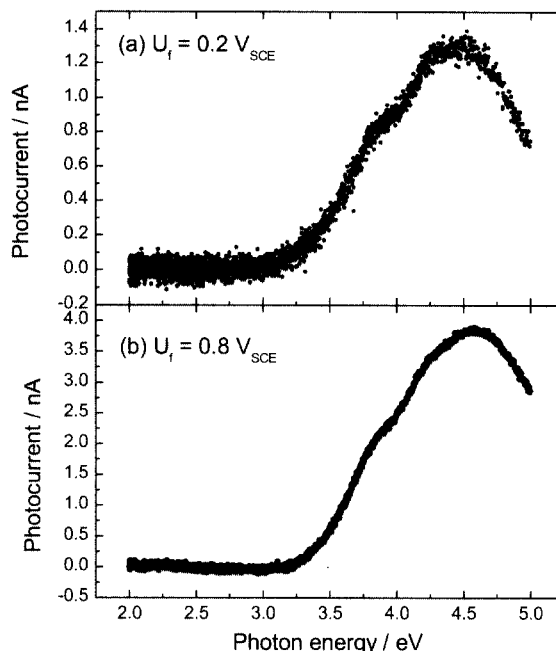


Fig. 1. i_{ph} vs. $h\nu$ plots for the passive film formed on Fe-20Cr (a) at 200 mV_{SCE} (a potential in the passive region) and (b) at 800 mV_{SCE} (a potential in the Cr-transpassive region) in deaerated pH 8.5 buffer solution.

3. Experimental results and discussion

3.1 Photoelectrochemical response

Typical photocurrent spectra for the passive film formed on Fe-20Cr at 200 mV_{SCE} (passive region) is presented in Fig. 1 (a), and it showed a close similarity with that for the passive film formed at 800 mV_{SCE} (Cr-transpassive region) that is shown in Fig. 1 (b). For both passive films, photocurrent began to increase at approximately 2.5 eV, exhibiting a shoulder at 3.8 eV with the peak current density at 4.5 eV. The anodic photocurrent confirms that the passive film formed on Fe-20Cr is an n-type semiconductor. The gradual increase in the photocurrent without sharp features on the photocurrent spectra is well known as the "Urbach tail", a characteristic of amorphous or highly disordered (or defective) semiconductor.¹²⁾ Passive films formed on Fe-20Cr at 0, 400, and 600 mV_{SCE} also showed the same photocurrent response as those depicted in Fig. 1.

According to the analytical results by AES, ISS, and XPS,²⁻⁵⁾ the passive film on Fe-Cr alloys is composed of Cr-enriched (Fe, Cr) oxide. For comparison, photocurrent spectra for the passive films formed on pure Fe and Cr in pH 8.5 buffer solution are presented in Fig. 2. It is clear that the photocurrent spectra for the passive film on Fe-20Cr closely resemble that for the passive film on pure

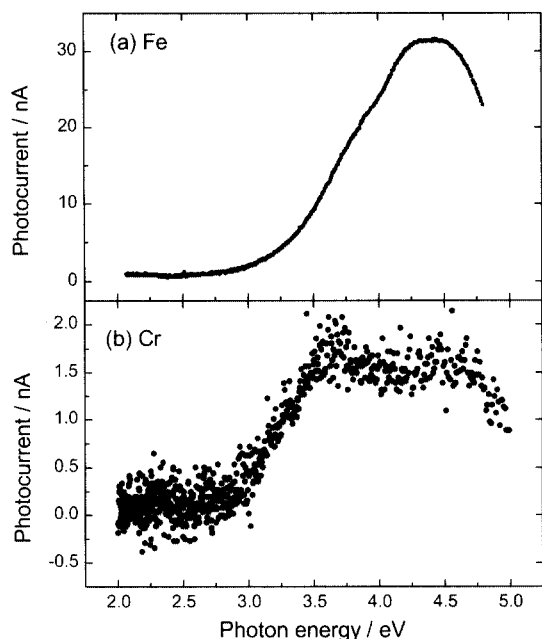


Fig. 2. i_{ph} vs. $h\nu$ plots for the passive film formed (a) on Fe at 400 mV_{SCE} and (b) on Cr at 300 mV_{SCE} in deaerated pH 8.5 buffer solution.

Fe except for the large difference in the photocurrent intensity; the photocurrent begins to increase at 2.5 eV, exhibits a shoulder and a subsequent peak at 3.8 eV and at 4.5 eV, respectively. These results demonstrate that the photocurrent of the passive film on Fe-20Cr is generated by the same electron transition sources occurring in the passive film on pure Fe, which are well agreed with the previous results reported by Ferreira et al.¹⁶⁾ They observed that Cr-oxide sputter-deposited on glassy carbon exhibited p-type semiconducting properties, whereas the sputter-deposited Cr-oxide on Fe substrate showed n-type semiconducting properties after annealing for 8 hr at 300°C.¹⁶⁾ Based on the results, they concluded that the Cr-oxide changed its p-type semiconducting properties to n-type ones similar to those of Fe-oxide by alloying with a small amount of Fe during the annealing. Thus, the semiconducting properties of the passive film on Fe-20Cr can be governed by the Fe-oxide even though it contains high concentration of Cr. In the previous photoelectrochemical study,¹⁵⁾ Kim et al. analyzed photocurrent responses for the passive film on Fe as a function of film formation potential, and suggested a modified band structure model based on that for crystalline spinel (γ -Fe₂O₃). Therefore, it can be inferred that the passive film on Fe-20Cr has a base structure of spinel γ -Fe₂O₃, (Cr-substituted γ -Fe₂O₃) and that the photo-assisted generation of electron-hole pairs in the passive film on the Fe-20Cr is originated by the d-d and p-d transitions. Recently, it has been de-

monstrated by *in situ* XANES and X-ray diffraction study¹⁾ that the passive film on Fe-Cr alloys has a spinel structure intermediate between that of Fe₃O₄ and γ -Fe₂O₃.

It should be noted from Figs 1 and 2 that the intensity of photocurrent for the passive film on Fe-20Cr is almost same as that of the passive film on pure Cr, but much lower than that for the passive film on pure Fe more than by one order of magnitude. This can be attributed to Cr³⁺ of the Cr-substituted γ -Fe₂O₃ constituting the passive film on Fe-20Cr and/or probably to a thinner passive film on Fe-20Cr than that on Fe. Analytical study showed that the passive film on Fe and Fe-Cr alloys has similar thickness.⁶⁾ Therefore, under the assumption that the absorption coefficient and quantum efficiency of the passive films on Fe and Fe-20Cr are similar, the Cr³⁺ in the passive film on Fe-20Cr may act as an efficient recombination site for electron-hole pairs generated by electron transition sources of γ -Fe₂O₃, thereby reducing considerably the photocurrent intensity for the passive film (Cr-substituted γ -Fe₂O₃) on Fe-20Cr.

Effect of presence of Cr³⁺ in the passive film on Fe-20Cr on the electronic properties of passive film can be explored further by investigating the change of photocurrent intensity with applied potential. If $\alpha \cdot L_h \ll 1$ and $\alpha \cdot W_{sc} \ll 1$, where α is light absorption coefficient of passive film, L_h is diffusion length of holes, and W_{sc} is thickness of the space charge layer, the intensity of photocurrent (i_{ph}) is a function of applied potential (U) according to Eq. (1);¹⁷⁾

$$i_{ph} = \alpha e J_0 \left(\frac{2\epsilon\epsilon_0}{eN_D} \right)^{1/2} (U - U_{FB})^{1/2} \quad (1)$$

where J_0 is the photon flux, e is electron charge, ϵ is the dielectric constant of the passive film taken as 15.6,¹⁴⁾ ϵ_0 is the permittivity of free space (8.854×10^{-14} Fcm⁻¹), N_D is the donor density, respectively, and U_{FB} is the flat band potential. α is a constant if incident photon energy is fixed. Fig. 3 shows a plot of i_{ph}^2 vs. U measured at the incident photon energy of 4.3 eV. The i_{ph}^2 has a linear relationship with U in accordance with equation (1) in the passive region (0-600 mV_{SCE}), and then increased abruptly in the Cr-transpassive region (800 mV_{SCE}). The abrupt increase in the photocurrent intensity at the Cr-transpassive potential shown in Fig. 3 appears to be caused by the decrease in the number of recombination sites resulting from the reduction of Cr³⁺ content due to the oxidation of Cr³⁺ to Cr⁶⁺ in transpassive region. In conclusion, the photocurrent of passive film on Fe-20Cr is generated by the electron transition sources of the Cr

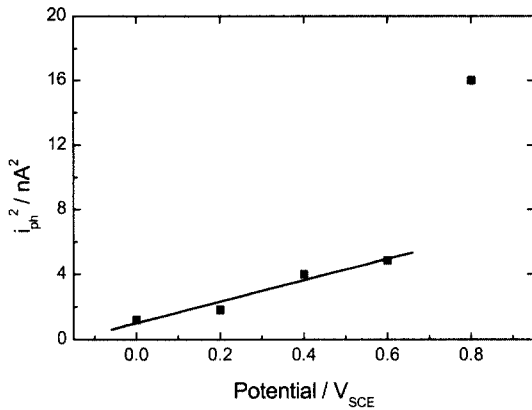


Fig. 3. i_{ph}^2 vs. applied potential plot for the passive film formed on Fe-20Cr in deaerated pH 8.5 buffer solution.

substituted γ -Fe₂O₃ involving the d-d and p-d transitions, and the conduction of the photo-generated electrons and holes is impeded by Cr³⁺ ions, acting as effective recombination sites of electron-hole pairs.

Band gap energy of the passive film can be obtained from Eq. (2) derived based on the assumption that the measured photocurrent is proportional to the optical absorption coefficient.

$$i_{ph} = A (h\nu - E_g)^n / h\nu \quad (2)$$

where A is a constant, $h\nu$ is energy of incident photon, E_g is the band gap energy, and n describes the type of transition between the valence and the conduction band in a crystalline material. In amorphous material, the same equation has been found as an empirical relation with n having different values, but predominantly 2.¹⁸⁾ The band gap energy for the film was determined by extrapolating the $(i_{ph} \cdot h\nu)^{1/2}$ vs. $h\nu$ plots with $n = 2$ to the axis of photon energy. The values of the band gap energy were 2.94 (3.07 eV and almost same irrespective of the film formation potential. The fact that the band gap energy is almost constant at various film formation potentials in the passive and Cr-transpassive region suggests that the band gap energy for the passive film is not affected by potential-dependent properties such as surface states, localized states deep in the band gap, etc.¹⁰⁾ Further, the passive film formed at potentials in the Cr-transpassive region has essentially identical structure with different Cr³⁺/Cr⁶⁺ content to that formed at potentials in the passive region, which is in a good agreement with the XANES results.¹¹⁾ A slight decrease or almost independence of band gap energy with increasing potential has also been observed by other authors.^{13),14)}

The value of the band gap for the passive film on Fe-20

Cr, obtained in this study (~3.0 eV), is same as that of the passive film on pure Fe in pH 8.5 buffer solution,¹⁶⁾ confirming again that the photocurrent response of passive film on Fe-20Cr is determined by the electron transition source occurring in spinel γ -Fe₂O₃, that is, the passive film on Fe. The previously reported band gap values for stainless steels is in the range of 1.9 ~ 3.6 eV.¹⁰⁻¹⁴⁾

3.2 Mott-Schottky analysis

The electronic properties of semiconducting passive film can be explored by measuring the capacitance of the space charge layer (C_{SC}) as a function of the electrode potential (U). The Mott-Schottky relationship expresses the potential dependence of C_{SC} of a semiconductor electrode under the depletion condition;¹⁹⁾

$$\frac{1}{C_{SC}^2} = \frac{2}{\epsilon \epsilon_0 e N_D} \left(U - U_{FB} - \frac{kT}{e} \right) \text{ or n-type semiconductor} \quad (3)$$

where e is electron charge, ϵ is the dielectric constant of the passive film, ϵ_0 is the permittivity of free space (8.854×10^{-14} Fcm⁻¹), N_D is the donor density, U_{FB} is the flat band potential, k is the Boltzman constant, and T is the absolute temperature. The value of N_D is determined from the slope of the experimental C_{SC}^{-2} vs. U plot by taking $\epsilon = 15.6$,¹⁴⁾ while U_{FB} from the extrapolation of the C_{SC}^{-2} vs. U plots to the U axis at $C_{SC}^{-2} = 0$. The Mott-Schottky relationship is based on the assumption that the capacitance of the space charge layer is much less than that of the Helmholtz layer.²⁰⁾ Normally Helmholtz capacitance of 25 ~ 50 μ Fcm⁻² satisfies this assumption.

Influences of film formation potential on the Mott-Schottky plot for the passive film formed on Fe-20Cr at potentials in the passive region (-100 to 600 mV_{SCE}) and in the Cr-transpassive region (700 to 900 mV_{SCE}) are presented in Fig. 4(a) and (b), respectively. The positive slopes of the Mott-Schottky plots indicate that the passive film formed on Fe-20Cr is an n-type semiconductor irrespective of the film formation potential. The Mott-Schottky plots for the passive film formed at potentials in the passive region showed one linear region, whereas those formed at potentials in Cr-transpassive region exhibited linear relationship in two potential regions. The second linear region appeared in the Mott-Schottky plots in Fig. 4(b) in the Cr-transpassive region is due presumably to the Cr⁶⁺ ions acting as a deep donor. The concentrations of the shallow and deep donors can be determined from slopes S_1 and S_2 of the two linear regions in the Mott-Schottky plots using the following equations;

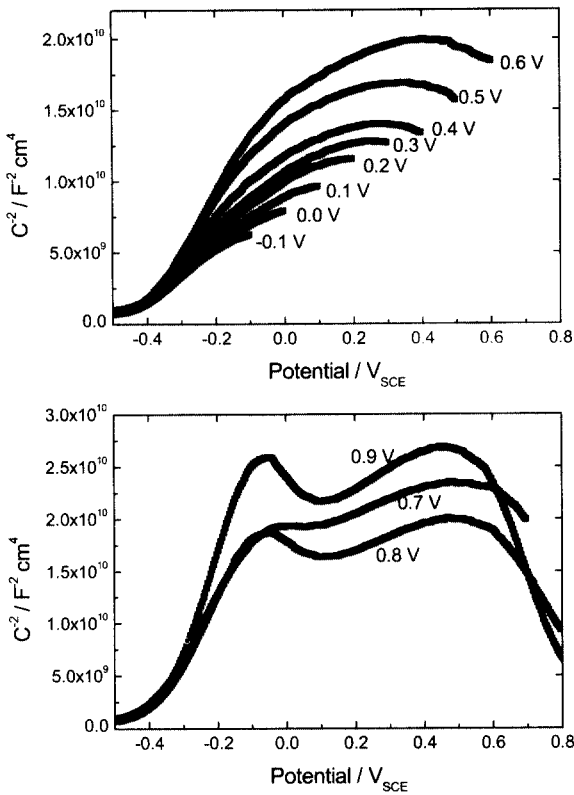


Fig. 4. Mott-Schottky plots for the passive film formed on Fe-20Cr at different potentials in deaerated pH 8.5 buffer solution. Capacitance was measured at 1000 Hz with a scan rate of 1 mV/s.

$$S_1 = \frac{2}{\epsilon\epsilon_o e N_{D1}} \quad \text{at lower potential region} \quad (4a)$$

$$S_2 = \frac{2}{\epsilon\epsilon_o e (N_{D1} + N_{D2})} \quad \text{at higher potential region} \quad (4b)$$

where N_{D1} and N_{D2} are the density of the donor at shallow and deep donor levels, respectively. The deep donors can be activated in the passive film formed at potentials in the Cr-transpassive region since Cr^{6+} ions produced at potentials noble to the Cr-transpassive potential (about 600 mV_{SCE}) became unstable with decreasing the potential, and eventually reduced to Cr^{3+} .

Hakiki et al.⁶⁾ reported, by assuming the duplex structure of inner Cr-oxide and outer Fe-oxide for the passive film on ferritic and austenitic stainless steels, that the Mott-Schottky behaviors in the potential range of -700 to -1200 mV_{SCE} were controlled by the inner Cr-oxide layer exhibiting p-type characteristics whereas those in the potential range of -400 to -100 mV_{SCE} by the outer Fe-oxide layer showing n-type one. However, the Mott-

Schottky response at potentials lower than -500 mV_{SCE} may be questionable, as they pointed out, because the passive film is unstable at such low potentials. There is large difference in the flat band potential between the inner Cr-oxide layer of the passive film on stainless steel and the passive film on pure Cr; -700 mV_{SCE} for the inner Cr-oxide of passive film⁶⁾ and 700 mV_{SCE} for the passive film on pure Cr.²¹⁾ In this work, we analyzed Mott-Schottky behaviors at potentials higher than -500 mV_{SCE}.

Fig. 5 shows the donor density as a function of film formation potential for the passive films formed on Fe-20Cr at various film formation potentials in the passive region and also in the Cr-transpassive region. The donor density (N_{D1} , N_{D2} , and $N_{D1} + N_{D2}$) decreased with increasing the film formation potential, which is well agreed with the previous results.^{13),22)} The order of magnitude of N_{D1} is 10^{20} cm^{-3} , which is in the same range of donor densities reported for the passive film formed on stainless

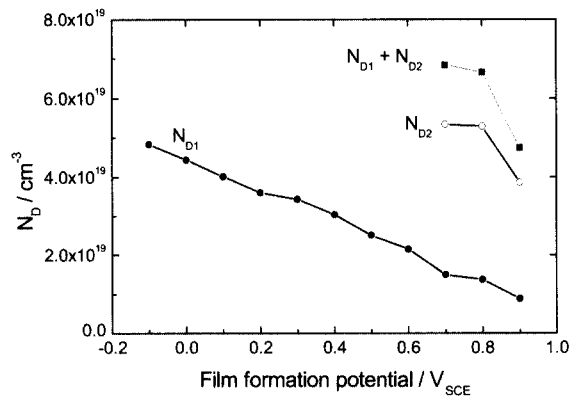


Fig. 5. Dependence of donor densities of shallow level (N_{D1}), deep level (N_{D2}) and total $N_{D1} + N_{D2}$ on film formation potential in deaerated pH 8.5 buffer solution.

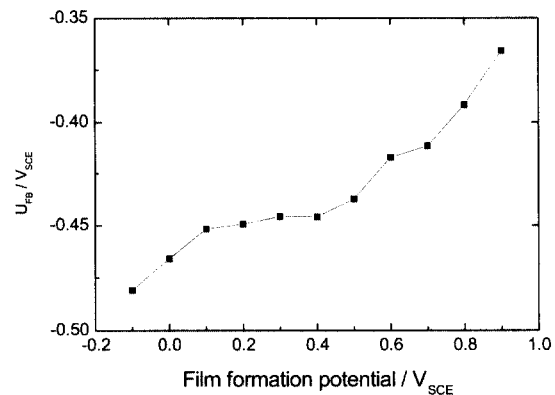


Fig. 6. Dependence of flat band potential (U_{FB}) of the passive film on film formation potential in deaerated pH 8.5 buffer solution.

steels.²²⁾ For passive films on iron base alloys, oxygen vacancy and metal interstitial are reported to act as donors.⁷⁾ Such a high donor concentrations also reflect the highly disordered nature of the passive film formed on Fe-20Cr. The flat band potential for the passive film on Fe-20Cr as a function of the film formation potential was obtained from the Mott-Schottky plots shown in Fig. 4, and presented in Fig. 6. The flat band potential increased from -480 mV_{SCE} to -360 mV_{SCE} as the film formation potential increased from -100 mV_{SCE} to 900 mV_{SCE}.

4. Conclusions

Electronic properties of the passive film formed on Fe-20Cr in pH 8.5 buffer solution were examined by photocurrent measurement and Mott-Schottky analysis. Conclusions drawn from this study are as follows:

1) The passive film formed on Fe-20Cr in pH 8.5 buffer solution is an amorphous or highly disordered n-type semiconductor, which was characterized by photocurrent spectra; anodic photocurrent, absence of sharp increase in the photocurrent spectra, and capacitance measurement; positive slope of Mott-Schottky plots and curved lines of Mott-Schottky plots.

2) The photocurrent spectrum for the passive films formed on Fe-20Cr was almost same in shape to that for the passive film of Fe, except for the large difference in photocurrent intensity, which demonstrated that the passive film on Fe-20Cr is composed of Cr-substituted γ -Fe₂O₃ involving the d-d and p-d electron transitions. However, the large difference in photocurrent intensity for passive film between Fe and Fe-20Cr may result from the fact that Cr³⁺ ions in passive film acts as effective recombination sites of electron-hole pairs.

3) The band gap energy of the passive film was measured to be ~3.0 eV, almost independent of film formation potential ranging from 0 to 800 mV_{SCE}.

4) With increasing film formation potential from -100 to 900 mV_{SCE}, the donor density of the passive film decreased from 5×10^{20} to 1×10^{20} cm⁻³ and the flat band potential increased from -480 to -370 mV_{SCE}.

5) The additional deep donor observed in Mott-Schottky plots for the passive film formed at potentials in Cr-transpassive region was associated with Cr⁶⁺ ions present in the film.

Acknowledgements

The authors gratefully acknowledge the financial su-

pport from Korea Science and Engineering Foundation (KOSEF), grant No. 97-0300-1001-3 and Department of Energy (DOE), grant No. DE-FG07-97ER62515.

References

1. L. J. Oblonsky, M. P. Ryan, and H. S. Isaacs, *J. Electrochem. Soc.*, **145**, 1922 (1998).
2. V. Mitrovic-Scepanovic, B. MacDougall, and M. J. Graham, *Corros. Sci.*, **24**, 479 (1984).
3. R. Kirchheim, H. Heine, H. Fischmeister, S. Hofmann, H. Knote and U. Stolz, *Corros. Sci.*, **29**, 899 (1989).
4. S. Haupt and H. -H. Strehblow, *Corros. Sci.*, **37**, 43 (1995).
5. V. Maurice, W. P. Yang, and P. Marcus, *J. Electrochem. Soc.*, **143**, 1182 (1996).
6. N. E. Hakiki, S. Bound, B. Randot, and M. Da Cunha Belo, *Corros. Sci.*, **37**, 1089 (1995).
7. D. D. Macdonald, *J. Electrochem. Soc.*, **139**, 3434 (1992).
8. P. Schmuki and H. Bohni, *Werkst. Korros.*, **42**, 203 (1991).
9. M. Bojinov, G. Fabricius, T. Laitinen, K. Makela, T. Saario, and G. Sundholm, *Electrochim. Acta*, **45**, 2029 (2000).
10. S. Fujimoto, O. Chihara, and T. Shibata, *Mat. Sci. Forum*, **289-292**, 989 (1998).
11. C. Sunseri, S. Piazza, A. Di Paola, and F. Di Quarto, *J. Electrochem. Soc.*, **134**, 2410 (1987).
12. A. Di Paola, F. Di Quarto, and C. Sunseri, *Corros. Sci.*, **26**, 935 (1986).
13. M. J. Klopfer, F. Bellucci, and R. M. Latanision, *Corrosion*, **48**, 229 (1992).
14. A. M. P. Simoes, M. F. S. Ferreira, B. Rondot, and M. Da Cunha Belo, *J. Electrochem. Soc.*, **137**, 82 (1990).
15. J. S. Kim, E. A. Cho, and H. S. Kwon, *Corros. Sci.*, **43**, 1403 (2000).
16. M. G. S. Ferreira, N. E. Hakiki, G. Goodlet, S. Faty, A. M. P. Simoes, and M. Da Cunha Belo, *7th International Symposium on Electrochemical Methods for Corrosion Research*, Key Note-08 (2000).
17. M. D. C. Belo, in *Electrochemical and Optical Techniques for the Study and Monitoring of Metallic Corrosion* (M. G. S. Ferreira and C. A. Melendres, eds), Kluwer Academic Publishers, Dordrecht, The Netherlands, 291 (1991).
18. N. F. Mott and E. A. Davis, in *Electronic Processes in Non-crystalline Materials*, Clarendon Press, Oxford (1979).
19. J. F. Dewald, *J. Phys. Chem. Solid*, **14**, 155 (1960).
20. R. De Gryse, W. P. Gomes, F. Cardon, and J. Vennik, *J. Electrochem. Soc.*, **122**, 711 (1975).
21. J. S. Kim, E. A. Cho, and H. S. Kwon, *The 8th International Symposium on the Passivity of Metals and Semiconductors*, May 9-14 (1999).
22. Y. F. Cheng and J. L. Luo, *Electrochim. Acta*, **44**, 2947 (1999).